(Received 12 December 2024, Accepted 24 February 2025, Scheduled 12 March 2025)

Quad-Port Staircase U-Shaped Wideband MIMO Antenna for 5G New Radio Applications

Sanket Nirmal[1], Sumit Kumar[1], and Richa Chandel[2,*]

[1] School of Electronics and Electrical Engineering, Lovely Professional University, Phagwara 144411, Punjab, India
[2] Department of Electronics and Communication Engineering, University Institute of Technology Himachal Pradesh University, Shimla 171005, India

ABSTRACT: This article introduces a quad-port Multiple Input Multiple Output (MIMO) staircase U-shaped wideband antenna for a 5G New Radio (NR) wireless. The miniaturization of the configuration is achieved with a staircase U-shaped radiating element, and an I-shaped stub etched with rectangular strips between radiating elements provides enhanced isolation. The measured bandwidth of 4.5 GHz is obtained with an isolation, radiation efficiency, and gain above 17 dB, 80%, and 6.5 dB respectively. Certain parameters, such as envelope correlation coefficient (ECC), diversity gain (DG), mean effective gain (MEG), channel capacity loss (CCL), and total active reflection coefficient (TARC), are also evaluated to ensure that the designed MIMO system adheres to its requirements. Hence, the suggested antenna suits the 5G New Radio applications.

1. INTRODUCTION

In today's wireless networks, Multiple Input Multiple Output (MIMO) antennas are essential for increasing data throughput and resolving signal problems. MIMO systems enable more effective data transmission, improve signal quality, and suppress interference and multipath fading. It also contributes to the progression of the efficiency and dependability of today's wireless communication networks. Further array configurations with MIMO technology increase channel capacity without requiring more bandwidth. Systems that demand low latency, high performance, or increased capacity can all benefit from the 5G network's improved service quality. The current scenario requirement is to develop a miniature MIMO antenna that can support several bands to enable the independent use of 5G NR bands in indoor networks, ensuring smooth transitions. Maintaining isolation between nearby deployed radiators is a significant difficulty for antenna designers since it adversely affects the MIMO's performance metric.

Improvements in the isolation between closely spaced antenna radiators have been reported using various methods [1–20]. In [1], with a dual-band capability antenna, the two-port MIMO antenna with asymmetrical T-shaped monopole and inverted E-shaped radiators meets the bandwidth requirements of the sub-6 GHz. In [2], it is stated that a linear array construction with two basic patch antennas demonstrated superior isolation and impedance matching without the need for traditional matching networks. In [3], at both lower and higher frequency bands, isolation is improved by an I-shaped decoupling structure between the radiating parts, exceeding 15 and 17 dB, respectively. In [4], the parasitic structures between the radiators efficiently minimized mutual coupling, increasing the isolation by 45 dB. In [5], a 4-element crescent ring-type slot and fractal geometry are utilized to create a notched band and an impedance matching at 4.6 GHz with a profile dimension of $60 \times 60 \times 1.6\,\text{mm}^3$. In [6], a patch and a ground slot were combined to create a better antenna design [7], resulting in enhanced isolation. But the CCL is relatively high in 3.0–5.7 GHz and 7.0–8.3 GHz band due to insufficient radiation efficiency. The operational range was increased using the complimentary split ring resonator (CSRR) approaches, and undesirable bands (3.5 and 5.5 GHz) were eliminated by using elliptical CSRR approach [8]. In [9], the operational band and the coupling between components have been increased by more than 22 dB by employing a substrate with a slotted edge. In [10], more than 23 dB of isolation was found for a tiny proximity-type microstrip antenna in isotropic radiation wireless applications. Moreover, antennas were positioned on both levels using the Kraus technique to increase bandwidth [11]. A staircase-shaped modified ground structure and an arc on the radiator followed the orthogonally positioned quad-element MIMO antenna, which showed the isolation of $S_{12} < -22$ dB and $S_{13} < -23$ dB [12]. A back-to-back slot with a twin port for WLAN of 2.4/5 GHz was utilized to implement the meander line design, which operates in dual bands for wireless LAN. A pair of slits was utilized to increase isolation and deliver the necessary value up to 17 dB [13]. In [14], using parasitic resonators and stub placement, a semi-elliptical structure was used to construct a four-element ultra-wideband (UWB) antenna isolated more than 20 dB. Additionally, different techniques including an electromagnetic bandgap (EBG), neutralization line (NL), and defective ground structure (DGS), are often employed. However, the maximum isolation is mostly attained in an EBG because of the increased capacitance, which leads to high efficiency and diversity gain [15]. In [16], the

* Corresponding author: Richa Chandel (richachandel25@gmail.com).

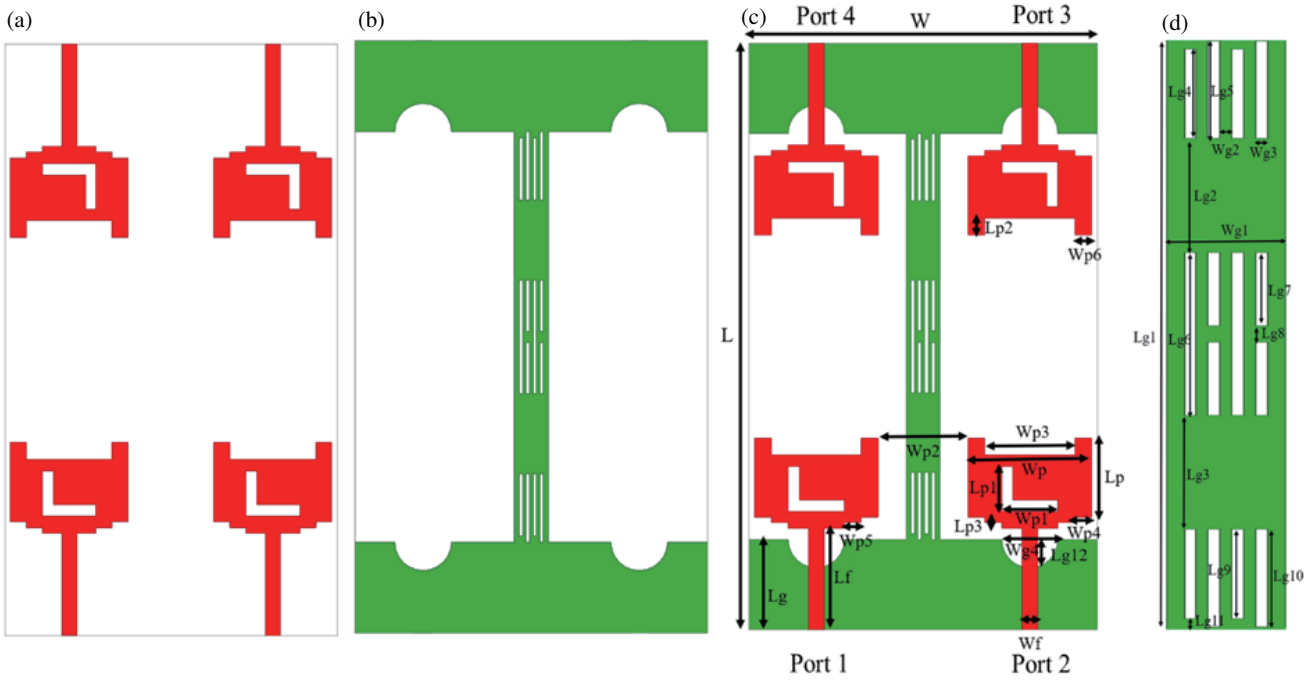

FIGURE 1. (a) Front view, (b) back view, (c) layout of the suggested MIMO antenna, (d) modified I-shaped structure dimension. (unit: mm, $L = 52$, $W = 31$, $W_p = 10$, $L_p = 12$, $W_f = 1.8$, $L_f = 9$, $L_{g12} = 2.12$, $L_g = L_{g3} = L_{g2} = 7$, $W_{p1} = 4$, $L_{p1} = 5$, $W_{p3} = L_{g5} = L_{g10} = 6$, $L_{p2} = 2$, $L_{p3} = W_{p4} = W_{p7} = L_{g8} = L_{p4} = 1$, $W_{p5} = W_{p6} = 2$, $L_{g1} = 38$, $W_{g1} = 3$, $h = 1.6$, W_{p2} =8, $L_{g4} = L_{g9} = 5.5$, $L_{g6} = 10$, $L_{g7} = W_{g4} = 4.5$, $L_{g11} = 0.5$, $W_{g2} = W_{g3} = 0.3$).

suggested hybrid strategy produced an adequate isolation value of 25 dB. In [17], high isolation was attained using the NL approach, which has a bandwidth variation of 3.52–10.08 and 23 dB of isolation [18].

However, the above structure has minimal isolation, poor coupling, and covers only partial sub-6 GHz 5G band. The coupling can be improved further by introducing metamaterial and CSRR structures and the isolation can be improved by using numerous tuning elements and the involvement of improved feedline which improves efficiency. Further, some array structures have very narrow bandwidth coverage of 5.35% at 5.5 GHz. Additionally, the gain is a major concern which can be improved by using low loss material and diverse gain enhancement techniques [14–28].

In this manuscript, we design and construct a quad-port MIMO antenna with a modified ground plane. A captivating feature of this structure is its miniaturization and high isolation. The staircase U-shape radiating element and an I-shape stub etched with rectangular strips between radiating elements provide enhanced isolation. It limits the amount of current flow from one element to another one to limit surface current. This configuration covers the requisite bandwidth of 5G NR. Fig. 1. shows the structure of the designed MIMO antenna.

2. ANTENNA CONFIGURATION AND ANALYSIS

2.1. Single Port Antenna

In this section, a single radiating element with an overall dimension of $26 \times 14 \times 1.6\,\text{mm}^3$ printed on an FR4 substrate is presented. The development of a single-element antenna with a modified ground plane, an L-shaped slot, and a U-type radiating patch is explained. The development of single-port antenna stages is illustrated in Fig. 2. Antenna 1 originates with a basic rectangular patch radiator consisting of partial ground, illustrated in Fig. 2. In antenna 2, the radiator is modified by etching uniform steps on the lower side, due to which the band occurs at a lower frequency of around 4.5 GHz. In antenna 3, the radiator is designed with a partial ground and a U-type slot on the upper side. It provides 4.7 to 9.46 GHz as its frequency range. Further, the radiator center has an L-shaped slit etched in it, and Fig. 2 shows a semi-circular slot in the partial ground. With these transformations, the recommended MIMO achieves the 5G band from 3.73 to 9.46 GHz at a 5.6 GHz resonant frequency.

2.2. Mathematical Modelling

According to [30, 31], the slot dimensions are given by Equation (1)

$$W = \frac{1}{2 \times f_r \times \sqrt{\mu} \times \epsilon_0} \times \sqrt{\frac{2}{\epsilon_r + 1}} \tag{1}$$

The substrate's constant is considered from Equation (2) as,

$$\epsilon_{reffp} = \frac{\epsilon_r + 1}{2} + \frac{\epsilon_r - 1}{2} \times \left[1 + 12 \times \frac{H_S}{W}\right]^{\frac{-1}{2}} \tag{2}$$

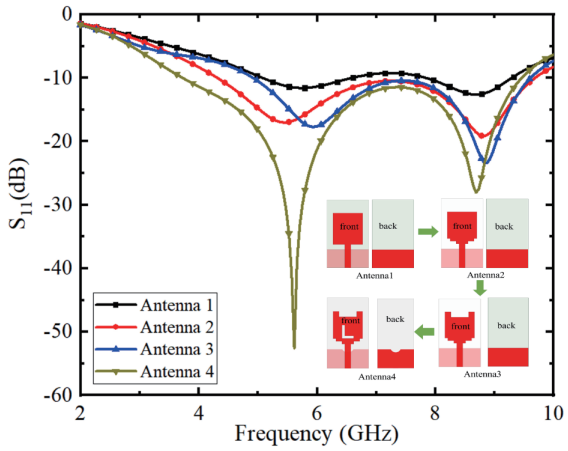

FIGURE 2. Effect of S_{11} due to development steps of single-element antenna.

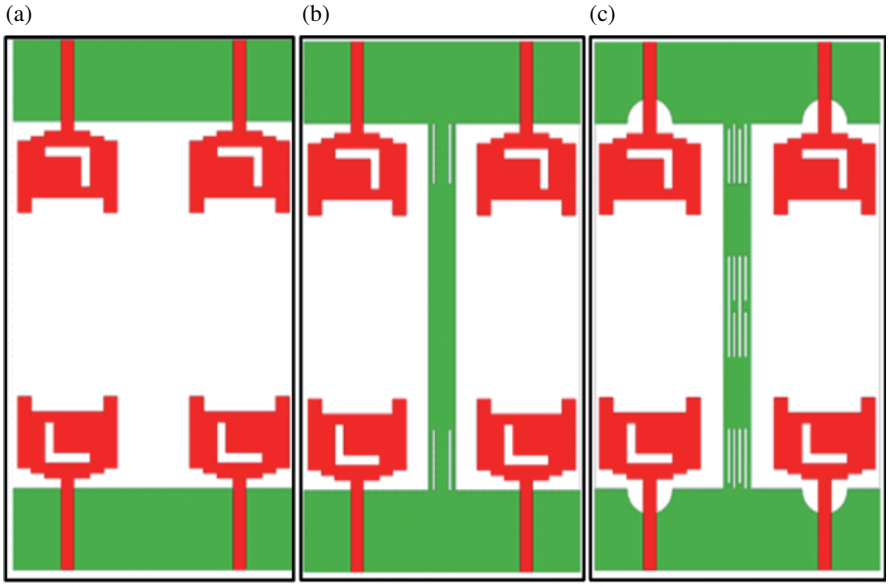

FIGURE 3. Evolution of isolation structure (a) without I-shaped (b) with I-shaped and corner slit (c) modified I-shaped.

Accordingly, Equation (3) calculates the antenna's length L.

$$\frac{\Delta L}{H_S} = 0.412 \times \frac{(\epsilon_{reffp} + 0.3)\left(\frac{W}{H_S} + 0.264\right)}{(\epsilon_{reffp} + 0.258)\left(\frac{W}{H_S} + 0.8\right)} \quad (3)$$

$$L = \frac{c}{2f_r\sqrt{\epsilon_{reff}}} - 2\Delta L \quad (4)$$

where f_r is the resonant frequency, ϵ_{reffp} the substrate effective constant, ϵ_r the substrate material constant, ΔL the extended length, W the slot width, H_S the substrate height, ϵ_0 free space permittivity, and c the speed of light (3×10^8 m/sec).

2.3. Quad Port MIMO Antenna

A single-port antenna may be transformed into a quad-port MIMO antenna with an expanded substrate and connected ground, as illustrated in Fig. 1. The size of the suggested MIMO antenna is $52 \times 31 \times 1.6\,\text{mm}^3$. The feeding mechanism comprises a $50\,\Omega$ microstrip-line feed in each radiator with a dimension of L_f and W_f. Here, a symmetric feed line creates four closely spaced, face-to-face, U-shaped rectangular radiators with a partial ground to increase the gain and bandwidth.

2.4. Evolution of Isolation Structure

This section analyses the performance of three distinct ground structures, as shown in Fig. 3. Fig. 3(c) shows how to achieve high isolation by placing an enhanced I-type stub between radiating components on the ground plane. The mutual coupling is achieved by introducing an I-shaped isolation structure and four rectangular strips on the ground plane between antenna elements to enhance the isolation. An I-shaped stub impedes the current flow between the adjoining elements of the antenna. The implementation of this efficient structure produces the isolation ($S_{12} < -15$ dB, $S_{13} < -20$ dB, $S_{14} < -15$ dB) among

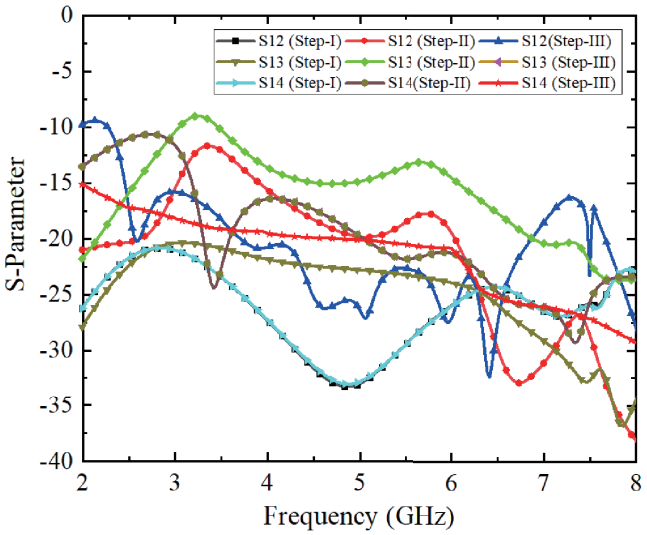

FIGURE 4. Effect of S-parameters due to isolation structures.

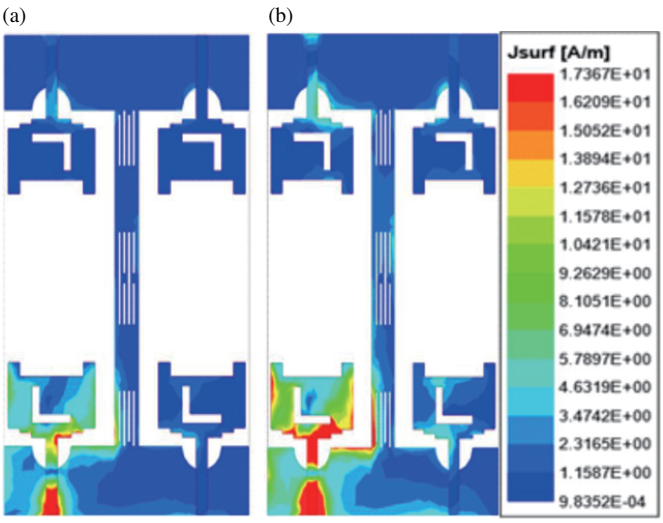

FIGURE 5. Surface current of quad-port MIMO at (a) 3.4 GHz (b) 5.2 GHz.

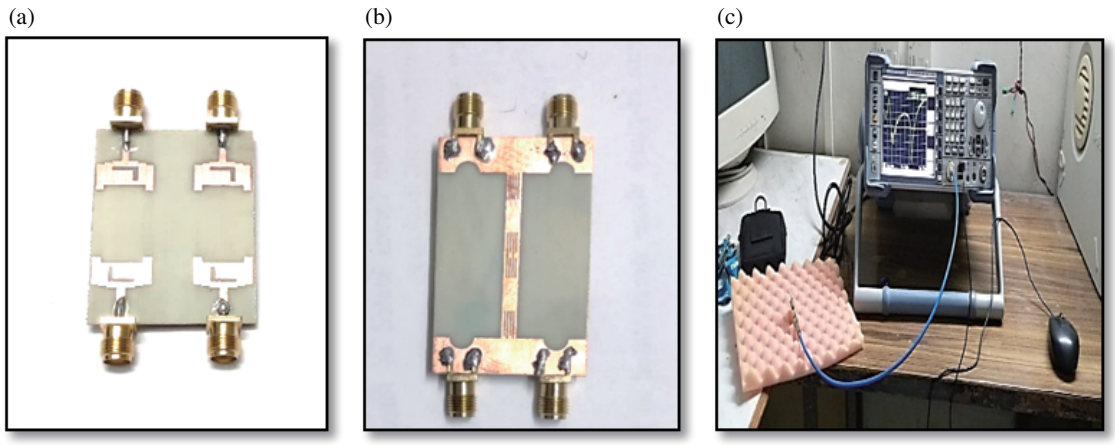

FIGURE 6. The photograph of fabricated suggested MIMO antenna. (a) Top view. (b) Bottom view, and (c) Measurement environment.

the antenna elements across the frequency band, as illustrated in Fig. 4.

The current circulation on the patch surface at 3.4 and 5.2 GHz is illustrated in Fig. 5. As per observation, the surface current occurs across the feeding line, and a small amount of current exists on the radiating patch and ground at a 3.4 GHz resonant frequency. A high surface current density occurs at 5.2 GHz because of the U-shaped slot etched on the radiating patch. When Port 1 is excited, and the other ports are matched with 50 Ω, no portion of the current is reached on the other elements. Hence, it shows that all the ports are isolated from each other.

3. EXPERIMENTAL ANALYSIS OF MIMO ANTENNA

The quad-port MIMO antenna's fabricated prototype is illustrated in Fig. 6. The measured and simulated S-parameters are illustrated in Fig. 7. The suggested MIMO antenna operates in the 5G NR bands range of 3.06 GHz to 7.56 GHz, with a bandwidth of 4.5 GHz, and the percentage of impedance bandwidth is 84.75%. The achieved isolation is above 17 dB in the operational band. The results obtained from the simulation and measurement coincide well. The measured value exhibits slight deviation, which is attributed to the cabling effect and SMA connector. The radiation efficiency and gain of the suggested antenna vary from 2 to 7 dBi and 90% to 95%, respectively, in the operational band, as illustrated in Fig. 8. The radiation patterns in the H-plane and E-plane at 3.4 and 5.2 GHz, as illustrated in Fig. 9, are observed to be directional. The H-plane patterns show a 180° phase dissimilarity. The omnidirectional and directional patterns are achieved at 3.4 and 5.2 GHz, respectively.

Table 1 provides a comparison between the proposed work and previous literature. The analysis shows that the fabricated prototype has compact dimensions with wide bandwidth coverage, sufficient isolation, and an excellent correlation coefficient useful for NR bands like n77, n78, and n79 as well as for WLAN bands (Wi-Fi-5 and Wi-Fi-6) applications.

TABLE 1. Comparison of the proposed work with other previously reported MIMO antennas.

Ref.	Antenna Electrical Size	No. of Antenna elements	Bandwidth (GHz)	Isolation (dB)	Gain	ECC
[14]	$0.679\lambda_g \times 0.730\lambda_g$	4	3.1–10.6	20	4	< 0.2
[15]	$0.617\lambda_g \times 0.617\lambda_g$	4	3.2–5.75	-22	9	< 0.05
[18]	$1.164\lambda_g \times 0.896\lambda_g$	4	5.15–5.85	20	2.8	NG
[21]	$2.85\lambda_g \times 1.39\lambda_g$	4	3.4–3.6, 4.8–5.0	17.5, 20	NG	< 0.14 < 0.12
[22]	$1.65\lambda_g \times 3.76\lambda_g$	4	5.6–5.67	> 30	NG	< 0.005
[23]	$1.64\lambda_g \times 0.82\lambda_g$	4	2.7–3.6	> 13	> 3	< 0.009
[24]	$2.87\lambda_g \times 1.44\lambda_g$	8	3.3–7.1	> 12	4.6–6.2	< 0.07
[25]	$2.96\lambda_g \times 1.48\lambda_g$	8	3.3–3.9	> 18	3	< 0.001
[26]	$3.04\lambda_g \times 1.62\lambda_g$	8	3.6–3.8, 5.15–5.92	> 15	> 3	< 0.2
[27]	$1.08\lambda_g \times 1.08\lambda_g$	4	3.26–5.18	< -15	2.5 & 4.5	< 0.005
[28]	$1.18\lambda_g \times 0.59\lambda_g$	8	5.15–5.92	< -10	12.6	< 0.005
[29]	$1.94\lambda_g \times 0.97\lambda_g$	4	3.4–3.8	> 20	5.21	0.005
Proposed	$\mathbf{0.97\lambda_g \times 0.58\lambda_g}$	**4**	**3.06–7.56**	$\mathbf{> 17}$	**7**	$\mathbf{< 0.0015}$

As, λ_g is guided wavelength.

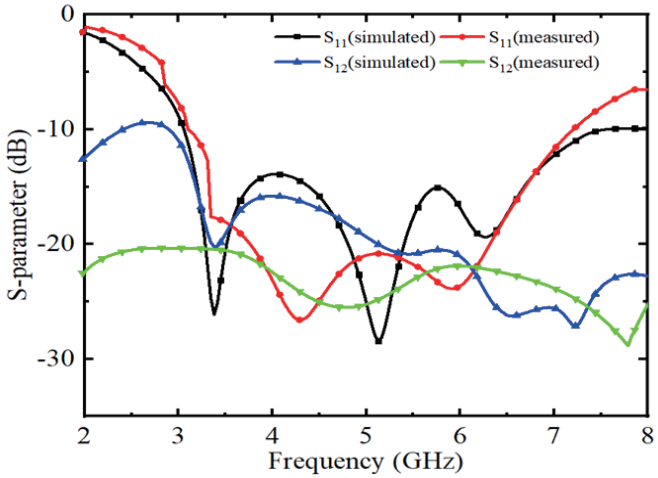

FIGURE 7. Measured and simulated S-parameters of the suggested MIMO antenna.

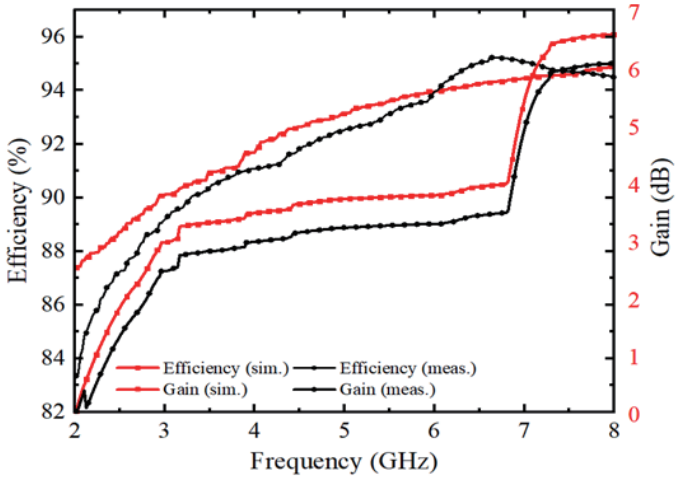

FIGURE 8. Measured and simulated efficiencies and gains of the suggested MIMO antenna.

4. DIVERSITY PERFORMANCE OF MIMO ANTENNA

The various diversity parameters of the MIMO antenna are analyzed through total active reflection coefficient (TARC), diversity gain (DG), channel capacity loss (CCL), mean effective gain (MEG), and envelope correlation coefficient (ECC) [5, 32].

To understand the behaviour of MIMO antenna, it is always essential to first verify individual antenna element performance for the parameter like correlation coefficient and diversity gain, determined from S-parameter. For higher antenna efficiency, the appropriate correlation is obtained with the help of S-parameters as shown in Fig. 10. The value of ECC in the operational bands is less than 0.05. Further, in wireless antenna communication, signal travels through multiple paths and results in the dissipation during power transmission through MIMO element without compromising loss of performance and thus, evaluated by diversity gain. The calculated DG from ECC are shown in Fig. 10, and Equations (5) and (6) show the expressions for ECC and DG.

TARC defines the radiation band of quad element MIMO antenna and is calculated through Equations (7) and (8) defined using S-parameters as in [29] and is always ≤ 10 dB. The result shows the shifting of frequency due to the imperfection in measured and simulated results caused by fabrication errors. The input signal to the port one is linear, and others are excited by deviation in phase angle. The channel capacity loss (CCL) esti-

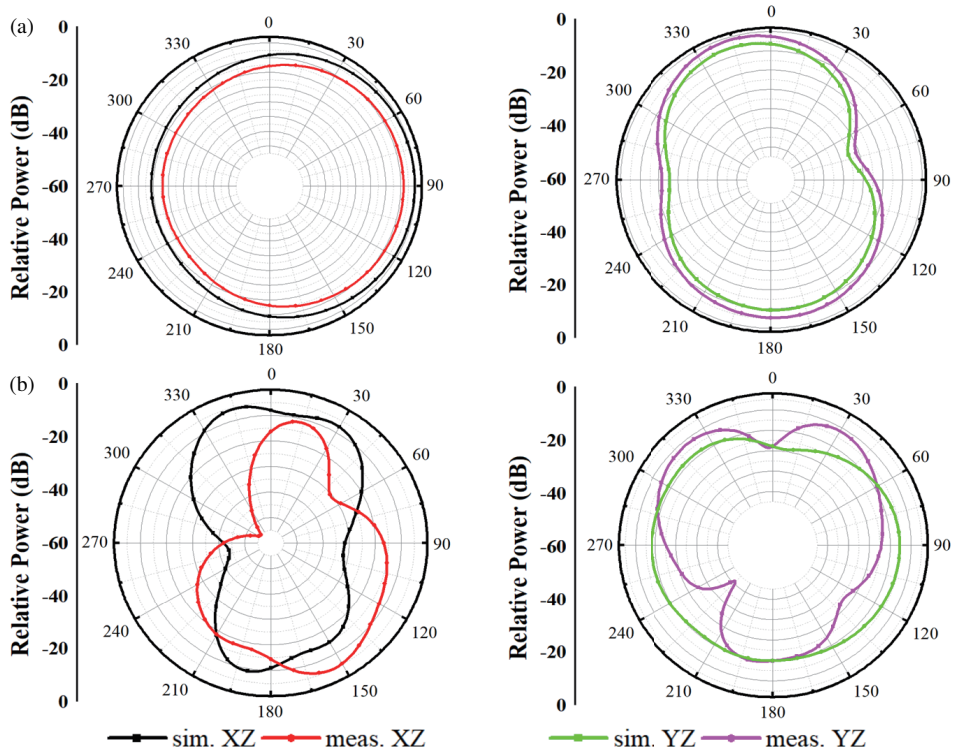

FIGURE 9. Radiation patterns in XZ and YZ-planes at (a) 3.4 and (b) 5.2 GHz.

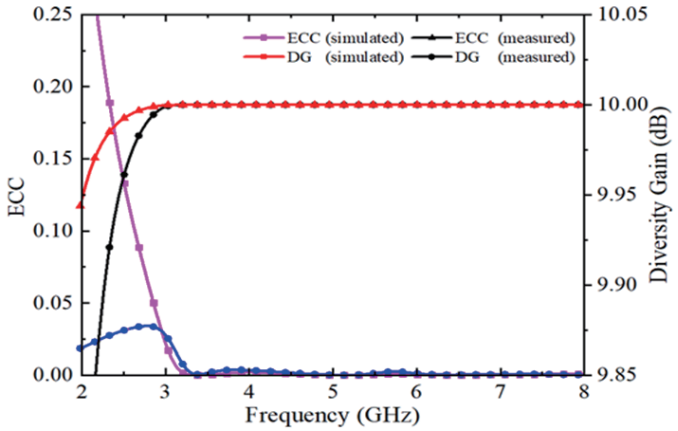

FIGURE 10. Measured and simulated ECCs and DGs of the suggested MIMO antenna.

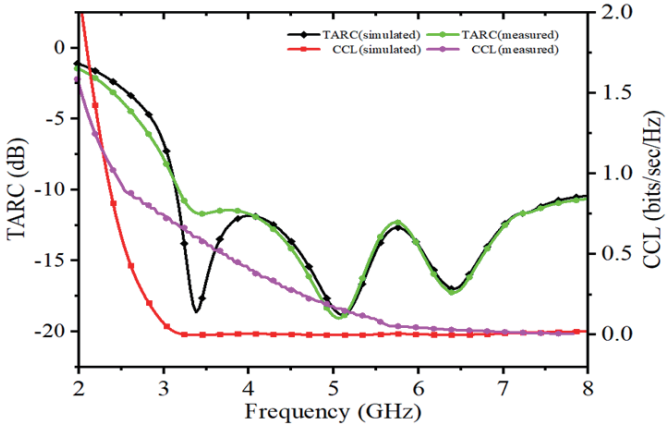

FIGURE 11. Measured and simulated TARCs and CCLs of the suggested MIMO antenna.

mated in fading environment by considering appropriate signal to noise power and calculated by admittance from port 1 to port 4 is well defined as [28, 29], and it is determined through Equations (9) to (15). For the simplicity, the analysis of port 1 and 2 is taken here. Figs. 10 and 11 illustrate the MIMO's diversity measurement metrics performance. The environmental effects have impact on the overall gain of antenna. MEG is the ratio of average power accepted to the power incident, has considerable rage of < -3 dB, and is shown in Fig. 12.

$$ECC_{m\times n} = \frac{|S_{11}^{*}S_{12}+S_{12}^{*}S_{22}+S_{13}^{*}S_{32}+S_{14}^{*}S_{42}|^{2}}{(1-(|S_{11}|^{2}+|S_{21}|^{2}+|S_{31}|^{2}+|S_{41}|^{2}))(1-(|S_{12}|^{2}+|S_{22}|^{2}+|S_{32}|^{2}+|S_{42}|^{2}))} \tag{5}$$

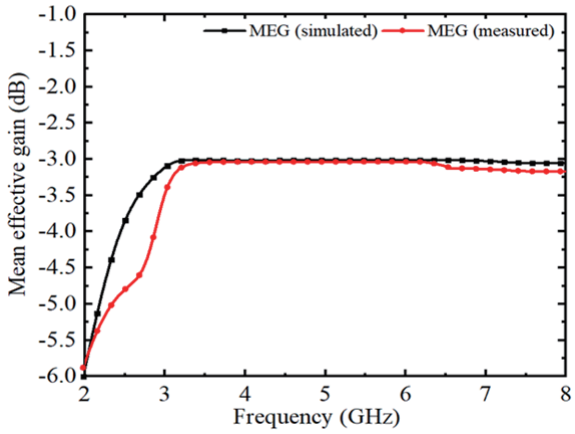

FIGURE 12. Measured and simulated MEGs of the suggested MIMO antenna.

$$DG_{m\times n} = 10\sqrt{1 - ECC^2_{m\times n}} \quad (6)$$

$$TARC_{m\times n} = \sqrt{\frac{(s_{mm}+s_{mn})^2 + (s_{nm}+s_{nn})^2}{2}} \quad (7)$$

$$TARC_{14} = \sqrt{\frac{(s_{11}+s_{14})^2 + (s_{41}+s_{44})^2}{2}} \quad (8)$$

$$C_{loss} = -\log_2 \det(Y^R) \quad (9)$$

$$\text{as, } (Y^R) = \begin{bmatrix} Y_{11} & Y_{12} \\ Y_{21} & Y_{22} \end{bmatrix} \quad (10)$$

$$Y_{11} = 1 - |s_{11}|^2 - |s_{12}|^2 \quad (11)$$

$$Y_{22} = 1 - |s_{22}|^2 - |s_{21}|^2 \quad (12)$$

$$Y_{12} = -[S^*_{11}S_{12} - S^*_{21}S_{12}] \quad (13)$$

$$Y_{21} = -[S^*_{22}S_{21} - S^*_{12}S_{21}] \quad (14)$$

As the expected value of ECC is below 0.5, in the proposed structure the obtained value of ECC is below 0.05 which is quite good. DG $>$ 9.999, MEG $<$ -3 dB, TARC $<$ 0.4, and CCL $<$ 0.2 bits/s/Hz indicate the superior MIMO performance parameters used efficiently for the fifth-generation application.

5. CONCLUSION

This article has suggested a quad-port staircase MIMO antenna for 5G-NR applications. High isolation and miniaturization, which are the crucial constraints for the MIMO system, have been attained only by the involvement of a staircase U-shaped radiating element and an I-shaped stub etched with rectangular strips in the ground plane. The beneficial part of this design is its compact size, which has a dimension of $52 \times 31\,\text{mm}^2$. The design has progressed through fabrication accompanied by a testing phase to estimate the uniformity of simulated and measured results. The stated design exhibits the results such as the gain of 6.5 dBi, 84.74% impedance bandwidth, isolation $<$ -17 dB, ECC $<$ 0.05, DG $>$ 9.999, $\text{MEG}_1/\text{MEG}_2 \geq 0.95$, TARC ≤ -10 dB, and CCL $<$ 0.2 bits/sec/Hz. Hence, we can simply claim that this design is a suitable candidate for 5G NR (n77/n78/n79) application in the Sub-6 GHz band as well as for WLAN (Wi-Fi 5 and Wi-Fi 6) band and imminent mobile communication.

REFERENCES

[1] Sim, C.-Y.-D., V. Dhasarathan, T. K. Tran, J. Kulkarni, B. A. Garner, and Y. Li, "Mutual coupling reduction in dual-band MIMO antenna using parasitic dollar-shaped structure for modern wireless communication," *IEEE Access*, Vol. 11, 5617–5628, 2023.

[2] Ghannad, A. A., M. Khalily, P. Xiao, R. Tafazolli, and A. A. Kishk, "Enhanced matching and vialess decoupling of nearby patch antennas for MIMO system," *IEEE Antennas and Wireless Propagation Letters*, Vol. 18, No. 6, 1066–1070, Jun. 2019.

[3] Liu, G., C. Zhang, Z. Chen, and B. Chen, "A compact dual band MIMO antenna for 5G/WLAN applications," *International Journal of Microwave and Wireless Technologies*, Vol. 14, No. 10, 1347–1352, 2022.

[4] Rekha, S. and S. R. J. Ramson, "Parasitically isolated 4-element MIMO antenna for 5G/WLAN applications," *Arabian Journal for Science and Engineering*, Vol. 47, No. 11, 14 711–14 720, 2022.

[5] Addepalli, T., M. S. Kumar, C. R. Jetti, N. K. Gollamudi, B. K. Kumar, and J. Kulkarni, "Fractal loaded, novel, and compact two-and eight-element high diversity MIMO antenna for 5G sub-6 GHz (N77/N78 and N79) and WLAN applications, verified with TCM analysis," *Electronics*, Vol. 12, No. 4, 952, Feb. 2023.

[6] Saritha, V. and C. Chandrasekhar, "A compact wide band MIMO antenna with quadruple notches in UWB," *Progress In Electromagnetics Research M*, Vol. 108, 237–247, 2022.

[7] Rekha, V. S. D., P. Pardhasaradhi, B. T. P. Madhav, and Y. U. Devi, "Dual band notched orthogonal 4-element MIMO antenna with isolation for UWB applications," *IEEE Access*, Vol. 8, 145 871–145 880, 2020.

[8] Raheja, D. K., B. K. Kanaujia, and S. Kumar, "Compact four-port MIMO antenna on slotted-edge substrate with dual-band rejection characteristics," *International Journal of RF and Microwave Computer-Aided Engineering*, Vol. 29, No. 7, e21756, 2019.

[9] Addepalli, T., "Compact MIMO diversity antenna for 5G Sub: 6 GHz (N77/N78 and N79) and WLAN (Wi-Fi 5 and Wi-Fi 6) band applications," *Wireless Personal Communications*, Vol. 132, No. 3, 2203–2223, 2023.

[10] Jayant, S. and G. Srivastava, "Compact 4 x 4 proximity coupled microstrip fed UWB stepped slot MIMO antenna having triple band rejection," *Wireless Personal Communications*, Vol. 119, No. 4, 3719–3734, 2021.

[11] Tirado-Méndez, J. A., H. Jardón-Aguilar, A. Rangel-Merino, L. A. Vasquez-Toledo, and R. Gómez-Villanueva, "Four ports wideband drop-shaped slot antenna for MIMO applications," *Journal of Electromagnetic Waves and Applications*, Vol. 34, No. 9, 1159–1179, Jan. 2020.

[12] Keshri, P. K., R. Chandel, S. K. Sahu, and A. K. Gautam, "Compact quad-port high performance UWB MIMO/diversity antenna with slotted ground structure," *Progress In Electromagnetics Research C*, Vol. 112, 193–205, 2021.

[13] Yang, Q., C. Zhang, Q. Cai, T. H. Loh, and G. Liu, "A MIMO antenna with high gain and enhanced isolation for WLAN applications," *Applied Sciences*, Vol. 12, No. 5, 2279, 2022.

[14] Amin, F., R. Saleem, T. Shabbir, S. U. Rehman, M. Bilal, and M. F. Shafique, "A compact quad-element UWB-MIMO antenna system with parasitic decoupling mechanism," *Applied Sciences*, Vol. 9, No. 11, 2371, Jun. 2019.

[15] Megahed, A. A., M. Abdelazim, E. H. Abdelhay, and H. Y. M. Soliman, "Sub-6 GHz highly isolated wideband MIMO antenna arrays," *IEEE Access*, Vol. 10, 19 875–19 889, 2022.

[16] Sharma, A., G. Das, and R. K. Gangwar, "Design and analysis of tri-band dual-port dielectric resonator based hybrid antenna for WLAN/WiMAX applications," *IET Microwaves, Antennas & Propagation*, Vol. 12, No. 6, 986–992, 2018.

[17] Khalid, M., S. I. Naqvi, N. Hussain, M. Rahman, Fawad, S. S. Mirjavadi, M. J. Khan, and Y. Amin, "4-Port MIMO antenna with defected ground structure for 5G millimeter wave applications," *Electronics*, Vol. 9, No. 1, 71, 2020.

[18] Cheng, Y., H. Liu, B. Q. Sheng, and L. Zhu, "A compact 4-element MIMO antenna for terminal devices," *Microwave and Optical Technology Letters*, Vol. 62, No. 9, 2930–2937, Sep. 2020.

[19] Tiwari, R. N., P. Singh, B. K. Kanaujia, and K. Srivastava, "Neutralization technique based two and four port high isolation MIMO antennas for UWB communication," *AEU — International Journal of Electronics and Communications*, Vol. 110, 152828, Oct. 2019.

[20] Kumar, P., A. K. Singh, R. Kumar, R. Sinha, S. K. Mahto, A. Choubey, and A. J. A. Al-Gburi, "High isolated defected ground structure based elliptical shape dual element MIMO antenna for S-band applications," *Progress In Electromagnetics Research C*, Vol. 143, 67–74, 2024.

[21] Ren, Z. and A. Zhao, "Dual-band MIMO antenna with compact self-decoupled antenna pairs for 5G mobile applications," *IEEE Access*, Vol. 7, 82 288–82 296, 2019.

[22] Khan, J., S. Ullah, F. A. Tahir, F. Tubbal, and R. Raad, "A sub-6 GHz MIMO antenna array for 5G wireless terminals," *Electronics*, Vol. 10, No. 24, 3062, 2021.

[23] Chattha, H. T., "4-port 2-element MIMO antenna for 5G portable applications," *IEEE Access*, Vol. 7, 96 516–96 520, 2019.

[24] Sghaier, N. and L. Latrach, "Design and analysis of wideband MIMO antenna arrays for 5G smartphone application," *International Journal of Microwave and Wireless Technologies*, Vol. 14, No. 4, 511–523, 2022.

[25] Parchin, N. O., Y. I. A. Al-Yasir, H. J. Basherlou, R. A. Abd-Alhameed, and J. M. Noras, "Orthogonally dual-polarised MIMO antenna array with pattern diversity for use in 5G smartphones," *IET Microwaves, Antennas & Propagation*, Vol. 14, No. 6, 457–467, 2020.

[26] Aziz, H. S. and D. K. Naji, "Compact dual-band MIMO antenna system for LTE smartphone applications," *Progress In Electromagnetics Research C*, Vol. 102, 13–30, 2020.

[27] Addepalli, T., T. Vidyavathi, K. Neelima, M. Sharma, and D. Kumar, "Asymmetrical fed Calendula flower-shaped four-port 5G-NR band (n77, n78, and n79) MIMO antenna with high diversity performance," *International Journal of Microwave and Wireless Technologies*, Vol. 15, No. 4, 683–697, 2023.

[28] Sim, C.-Y.-D., H.-Y. Liu, and C.-J. Huang, "Wideband MIMO antenna array design for future mobile devices operating in the 5G NR frequency bands n77/n78/n79 and LTE band 46," *IEEE Antennas and Wireless Propagation Letters*, Vol. 19, No. 1, 74–78, 2020.

[29] Kaushal, V., A. Birwal, and K. Patel, "Diversity characteristics of four-element ring slot-based MIMO antenna for sub-6-GHz applications," *ETRI Journal*, Vol. 45, No. 4, 581–593, 2023.

[30] Rai, J. K., P. Ranjan, S. Kumar, R. Chowdhury, S. Kumar, and A. Sharma, "Machine learning-enabled two-port wideband MIMO hybrid rectangular dielectric resonator antenna for n261 5G NR millimeter wave," *International Journal of Communication Systems*, Vol. 37, No. 16, e5898, 2024.

[31] Tiwari, P., J. K. Rai, V. Gahlaut, and P. Ranjan, "Compact quad element dual band high gain MIMO rectangular dielectric resonators antenna for 5G millimeter wave application," *AEU — International Journal of Electronics and Communications*, Vol. 178, 155280, 2024.

[32] Rai, J. K., P. Ranjan, R. Chowdhury, and M. H. Jamaluddin, "Design and optimization of dual port dielectric resonator based frequency tunable MIMO antenna with machine learning approach for 5G new radio application," *International Journal of Communication Systems*, Vol. 37, No. 13, e5856, 2024.